# High-Power Sources of Ultrawideband Radiation with Subnanosecond Pulse Length

A.M. Efremov, V.I. Koshelev, B.M. Kovalchuk, V.V. Plisko, K.N. Sukchushin

*Institute of High Current Electronics SB RAS, 2/3 Academichesky Ave., Tomsk, 634055, Russian Federation, Ph: (3822) 491-915, Fax: (3822) 492-410, e-mail: koshelev@lhfe.hcei.tsc.ru*

**The sources of high-power ultrawideband electromagnetic pulses with subnanosecond pulse length are presented. A bipolar voltage pulse of the length 0.5 ns and the amplitudes of -160/+200 kV was applied to the radiating system input (16-element array or single antenna). The efficient potential values $E_pR$ = 260 kV and $E_pR$ = 690 kV were obtained for a source based on a single antenna and for a source based on a 16-element array antenna, respectively.**

## 1. Introduction

The paper presents the sources of high-power ultrawideband electromagnetic pulses of subnanosecond pulse length. The sources (Fig.1) consist of a monopolar pulse generator (MPG) (1), a bipolar pulse former (BPF) (2) and a radiating system. A 16-element array antenna (5) excited from the BPF through the wave transformer (WT) (3) and power divider (4) or a single antenna (not presented in the Figure) can be used as a radiating system.

## 2. Bipolar pulse generator

A high-voltage pulse generator SINUS-160 was used in this source as a MPG. The electrical length of the generator line (double wave run) is 4.5 ns, the wave impedance is 40 Ohm and the charging voltage at a 100-Hz frequency is 360 kV [1].

A BPF is made by the scheme with an open-circuit line. In difference from the works [1,2], one more sharpening section is used to increase the rate of voltage rise at the discharge switch electrodes. The scheme was simulated at a personal computer by the program PSpice. The equivalent scheme of a BPF with the forming line of a MPG is shown in Fig. 2. Parameters of lines, inductors, resistors as well as the discharge switch turn-on time are presented here. The turn-on time of a discharge switch, i.e., the time during which the discharge switch impedance changes from 100 kOhm to 0.01 Ohm is established for S0, S1, S2 and S3 to be equal to 1; 0.75; 0.1 and 0.1 ns, respectively. Resistor R2 is necessary only for providing the program operation.

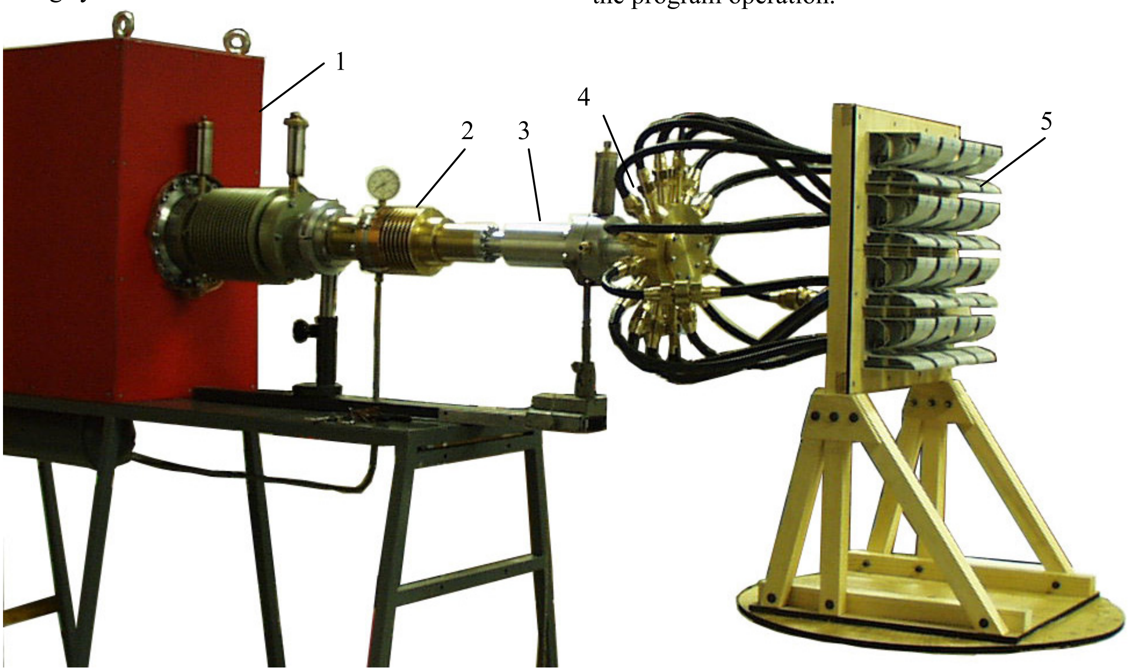


Fig.1. The external view of the radiation source. 1 – monopolar pulse generator, 2 – bipolar pulse former, 3 – wave transformer, 4 – power divider, 5 – 16-element array antenna.

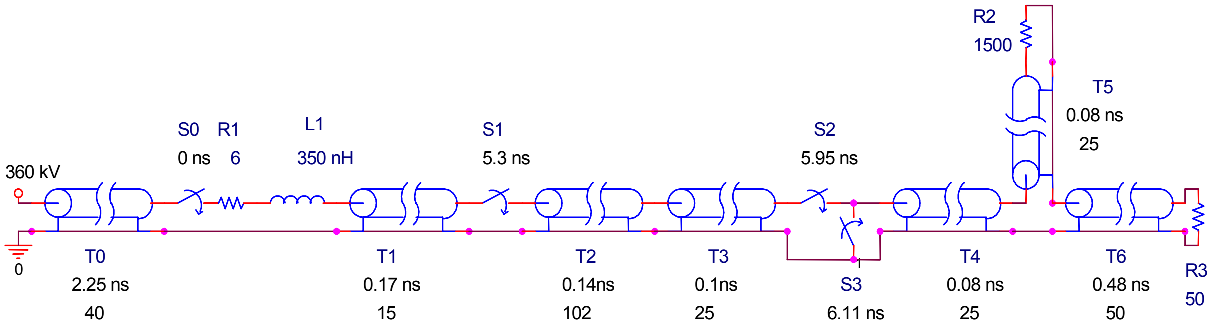


Fig.2. Equivalent circuit of a bipolar pulse former with MPG forming line.

The forming line T0 of the MPG charged to the voltage of 360 kV is commutated by the discharge switch S0 to the intermediate line T1 through the limiting resistor R1 = 6 Ohm and charging inductance L1 = 350 nH. The value of the charging inductance L1 was chosen so that the charging voltage at the line T1 close to the maximum one at the minimum time of charging from the MPG should be provided. The charging voltage U1 at the intermediate line T1 reaches ≈ 584 kV during ≈6.5 ns (Fig. 3). The discharge switch S1 operates in the charging voltage maximum and connects the line T1 through the high-impedance line T2 to the forming line T3 that is charged up to the voltage of ≈790 kV during the time of ≈0.5 ns (curve U3). A bipolar voltage pulse U6 with the amplitudes of ≈ 360 kV and pulse length of ≈0.5 ns is formed at operation of the discharge switch S2 in the charging voltage maximum at the line T3 and the discharge switch S3 with relative delay of 0.16 ns in the transmitting line T6 at the end of which the load R3 = 50 Ohm is installed.

A BPF design is presented in Fig. 4. The charging inductor L1, six coaxial lines T1-T6, the sharpening discharge switches S1-S2 and the cut-off discharge switch S3 are placed inside a massive brass case in the nitrogen medium under the pressure of 8.6 MPa. The charging inductor L1 is connected via the feed-through polyamide insulator with the limiting resistor R1 of the MPG. The line T5 has plexiglass insulation

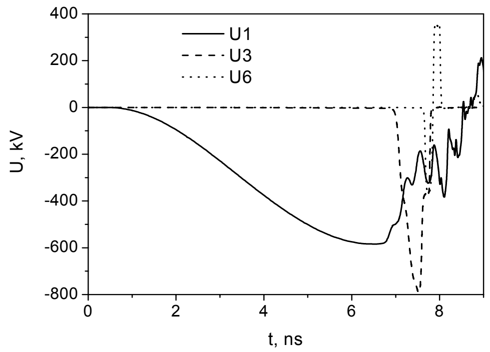


Fig.3. Calculated voltage pulses at the lines T1, T3, and T6.

and the lines T4, T6 have the ones made of fluoroplastic-4. Fig. 2 presents parameters of the lines, inductance, and resistive load. Diameters of the external conductors of the lines T1-T6 are equal to 35; 35; 23; 35; 16.5 and 35 mm, respectively. The ends of the internal conductors of the lines T1–T4 serve as the electrodes of the discharge switches S1 and S2. The internal conductor of the line T4 and the 2-mm thick disk at the external conductor of this line serve as electrodes of the cut-off discharge switch S3. All electrodes of the discharge switches are made of copper and the line conductors are made of brass. The gaps in the discharge switches S1 and S2 are adjusted by gaskets and equal to 1.55 and 1.25 mm, respectively. The transmitting line T6 connects the

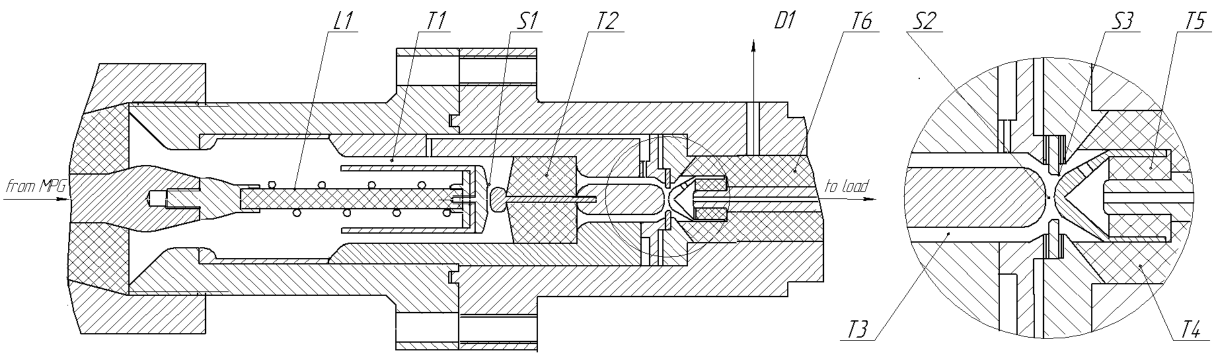


Fig.4. The bipolar pulse former design.

BPF output with the resistive load R3 (not presented in Fig.4). The output bipolar voltage pulse was recorded by the coupled-line voltage divider D1 installed in the line T6 by means of the oscilloscope TDS 6604. At the pulse repetition rate of 100 Hz the measured output bipolar pulse presented in Fig.5 has the amplitudes equal to -160; +200 kV and the pulse length of ≈0.5 ns at the level of 0.1 of the amplitudes.

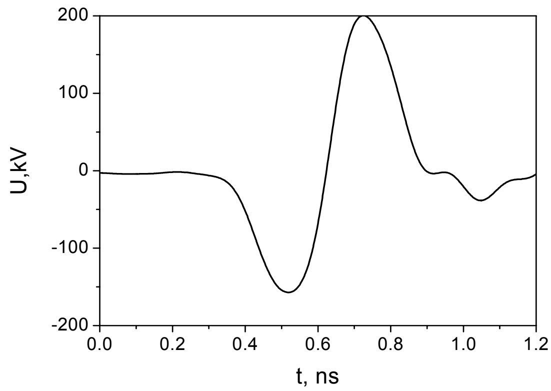


Fig.5. The measured voltage pulse at the former output.

Relative spread of the bipolar pulse amplitude doesn't exceed 4–5% at the relative spread of the charging voltage amplitude of SINUS-160 generator being less than 1%.

A wave transformer was used to match the BPF output wave impedance equal to 50 Ohm and the summary wave impedance of the array antenna feeder equal to 3.125 Ohm. Calculation by the program PSpice shows that the bipolar voltage pulse at the WT output begins distorting at the electric length of the transition $\tau \leq 0.6$ ns. At $\tau = 0.8$ ns, the calculated voltage pulse at the WT output has the waveform presented in Fig.6.

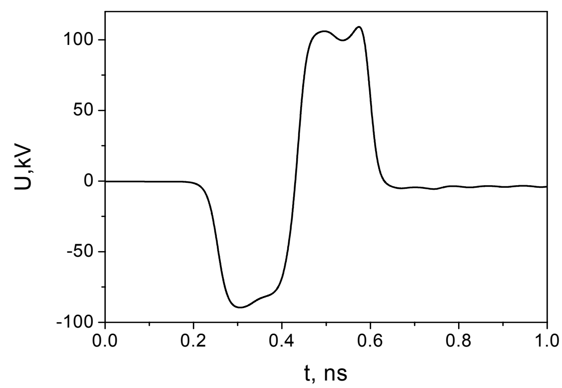


Fig.6. Calculated voltage pulse at the output of the wave transformer.

The WT design presents an oil-filled coaxial with the length of 153 mm. The wave impedance $\rho_w$ of the WT changes along the axis z by the law $\rho_w = 50 \exp(-18.22z)$. Diameters of the external conductors at the WT input and output are equal to 20 and 68 mm, respectively. The transformer input is connected to the BPF output through a polycarbone feedthrough insulator and its output is connected to a 16-channel power divider. A bipolar voltage pulse is applied from the WT to the array antenna by means of the cables of the PK-50-11-11-type. A capacitive voltage divider is installed in one of the cables to record the output pulse from the WT.

### 3. Radiating system

A combined antenna developed specially for the exciting bipolar pulse of 0.5 ns length was used both as a single radiator and an array element. The antenna is close in its design to the one described in Ref. [3] but has less dimensions of approximately 7.5×7.5×8 cm. In the source with a single antenna it was connected to the BPF output without using the WT and power divider. To prevent electrical breakdown, the antenna was placed into a dielectric container filled with $SF_6$-gas under the pressure of 0.4 MPa. In the array, the combined antennas are fastened at a dielectric plate at a 9-cm distance from each other. Designs of the inputs of a single antenna and an array element are different.

Fig.7 presents VSWR of a single antenna and an array element. Fig. 8 presents the patterns by the peak power in the H- and E-planes.

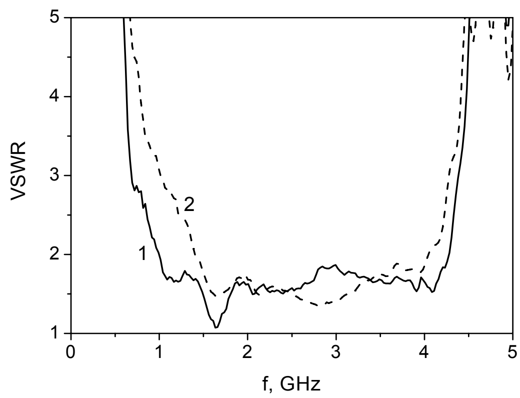


Fig.7. VSWR of a single antenna (1) and an array element (2).

The pattern width by the half-power level is equal to ~ 85° and ~ 110° in the H- and E-planes, respectively. If the antenna efficiency by energy and the space-time radiation characteristics are known, one can find the antenna efficiency by the peak power $k_p = P_{rad}/P_g$, где $P_{rad}$ is the peak power of radiation pulse, $P_g$ is the peak power of the generator voltage pulse at the antenna input. Measurements carried out at the antenna excitation by a low-voltage 0.5-ns bipolar pulse gave the value $k_p \approx 0.8$. The measured directivity factor of the antenna was D ≈4.

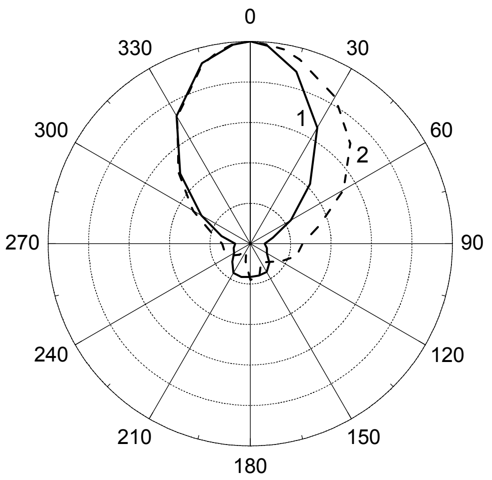


Fig.8. Combined antenna patterns in the planes H (1) and E (2).

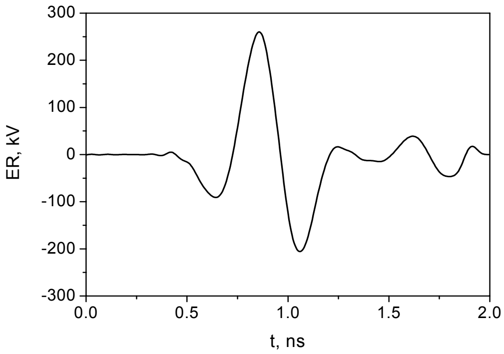


Fig.9. Waveform of the pulse radiated by the single antenna.

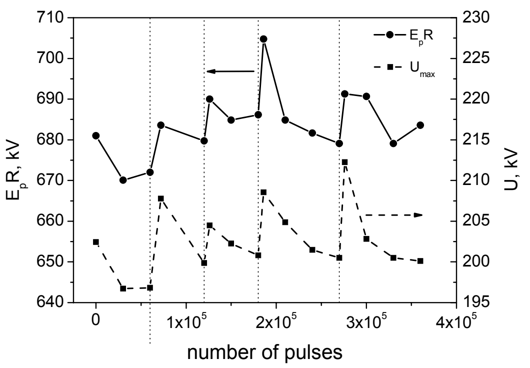


Fig.10. The bipolar voltage pulse amplitude and efficient potential versus the number of pulses.

### 3. Radiation of high-power ultrawideband pulses

Fig.9. presents the waveform of the electromagnetic pulse radiated by the single antenna. The efficient potential $E_pR$ was 260 kV, here $E_p$ is the peak electric field strength measured in the far-field zone at the distance R = 10 m. The root-mean-square deviation of $E_pR$ during 100 pulses was not higher than 5%.

Fig.10 presents the amplitude of the bipolar voltage pulse at the BPF output and efficient potential versus the number of pulses at the pulse repetition rate of 100 Hz for the source with a 16-element array. Vertical dotted lines in the diagram show the moments when 10-minute pauses were made in the generator operation in order to cool the BPF. The average value of the efficient potential was $E_pR \approx 690$ kV. The root-mean-square deviation of $E_pR$ during 100 pulses was not higher than 5% and the amplitude change during $3.6*10^5$ pulses (1 hour of operation) was not higher than 10%.

### Conclusion

The sources of ultrawideband radiation pulses with subnanosecond pulse length and ~600-MW peak power at the pulse repetition rate of 100 Hz have been developed. The efficient potential of the source with a 16-element array achieves 700 kV at the instability less than 10%. A BPF can operate continuously during one hour at the pulse repetition rate of 100 Hz if air cooling is used.

The work was partially supported by Russian Fund of Basic Research (Project No. 06-08-00295).

### References

[1] Yu.A. Andreev, V.P. Gubanov, A.M. Efremov, V.I. Koshelev, S.D. Korovin, B. M. Kovalchuk, V.V. Kremnev, V.V. Plisko, A.S. Stepchenko, K.N. Sukhushin, Laser and Particle Beams **21**, 211 (2003).

[2] V.P. Gubanov, A.M. Efremov, V.I. Koshelev, B. M. Kovalchuk, S.D. Korovin, V.V. Plisko, A.S. Stepchenko, K.N. Sukhushin, Instruments and Experimental Techniques **48**, 312 (2005).

[3] V.I. Koshelev, Yu.I. Buyanov, Yu.A Andreev, V.V. Plisko, K.N. Sukhushin, *in Proc. IEEE Pulsed Power Plasma Science Conf.*, 2001, vol.2, pp.1661-1664.